IEEE Access
Multidisciplinary | Rapid Review | Open Access Journal

Received June 2, 2020, accepted July 7, 2020, date of publication July 10, 2020, date of current version July 22, 2020.

*Digital Object Identifier 10.1109/ACCESS.2020.3008417*

# Design of Graphene-Based Dual-Polarized Switchable Rasorber/Absorber at Terahertz

**MEIJUN QU[1], (Student Member, IEEE), TIANYU CHANG[2], GAN GUO[3], AND SHUFANG LI[4], (Senior Member, IEEE)**

[1]School of Information and Communication Engineering, Communication University of China, Beijing 100024, China
[2]International Department, The State Radio_monitoring_center Testing Center, Beijing 100041, China
[3]China Telecommunication Technology Labs, China Academy of Information and Communications Technology, Beijing 100191, China
[4]School of Information and Communication Engineering, Beijing University of Posts and Telecommunications, Beijing 100876, China

Corresponding author: Gan Guo (guogan@caict.ac.cn)

This work was supported in part by the National Natural Science Foundation of China under Grant 61701448, and in part by the National Science and Technology Major Project of the Ministry of Science and Technology of China under Grant 2018ZX03001030.

**ABSTRACT** This paper reports a dual-polarized graphene-based multi-functional device which could switch between rasorber and absorber flexibly. The only difference between rasorber and absorber is that rasorber has a transmission window with low loss. Therefore, a wideband absorber is proposed at the first step. Then, four split-ring resonators (SRRs) are introduced to the absorber, which makes the electromagnetic (EM) energy could be reflected at the certain frequency band. The state (on/off) of SRRs and absorber can be controlled by the chemical potential of graphene. To find a new pathway for this part of the reflected energy, metal ground of the absorber is replaced by a reconfigurable graphene-based frequency selective surface (FSS). The proposed FSS could be switched between FSS and metal plate by controlling the chemical potential of graphene ring embedded in the bottom metal layer. Therefore, the proposed multi-functional device could be obtained by combing the absorber with SRRs and reconfigurable FSS. When the proposed device serves as a rasorber, it has an absorption-transmission-absorption response with superior selectivity. When it performs as an absorber, it has wideband performance with high absorptive rate. It is an attractive candidate for stealth applications.

**INDEX TERMS** Absorber, graphene, multi-functional, rasorber, switchable.

## I. INTRODUCTION

Frequency selective surface (FSS) radome allows EM waves to transmit in the transmission band and reflect the EM waves out-of-band [1]–[3]. FSS can reduce mono-static radar cross section (RCS) greatly. Nevertheless, the reflected wave by FSS increases scattering in other directions, which could be detected by bistatic/multistatic radar [4]. Nowadays, frequency-selective rasorber has been studied since rasorber can pass EM waves in the passband and absorb EM waves outside the passband. By this way, both mono-static and bistatic out-of-band RCS can be reduced. Therefore, rasorber has superior performance over conventionally used FSS in reducing RCS.

There are two classes of rasorbers, including three-dimensional [5], [6] and two-dimensional rasorbers [7]–[9] respectively. Three-dimensional rasorber could readily achieve high selectivity and angular-stable performance. Nevertheless, they are difficult to fabricate and assemble, especially in terahertz band. Thus, two-dimensional rasorber, usually consisting of a resistive sheet and a band-pass FSS, is designed in this paper. A dual-polarized band-absorption rasorber is presented in [10], achieving a high-frequency absorption and low-frequency bandpass performance. In [11], a miniaturized frequency-selective rasorber is designed with a wide absorption band below the transmission band. The above designs only have one absorption band near the passband. It would be more ideal if the rasorber has two absorption bands on the both sides of the passband. A dual-polarization frequency selective rasorber is proposed in [12] by combining split ring resonators and Jerusalem crosses. A broadband and high-selectivity rasorber based on notch structure is designed in [13]. These designs can realize a passband and two absorption bands. Nevertheless, the operating performance will be fixed once the device is fabricated.

With the development of wireless communication, it is becoming attractive to study multi-functional devices. In [14], a reconfigurable rasorber is presented. It could offer transmission or reflection band along with an absorption band

The associate editor coordinating the review of this manuscript and approving it for publication was Flavia Grassi.

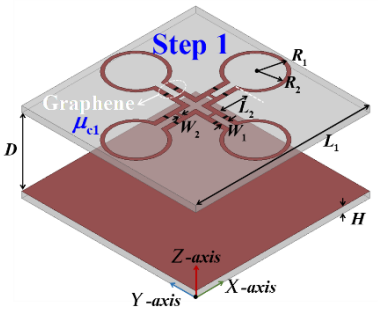


**FIGURE 1.** **Configuration of the proposed wideband absorber based on graphene.**

by changing the DC voltage applied in the bias network. In [15], a varactor-based rasorber is designed which could provide a tunable transmission window within the absorption band. Aforementioned designs are all in the microwave band. A graphene-based polarization insensitive rasorber is presented with tuneable passband at terahertz, achieving a switchable broadband frequency-selective rasorber/absorber [16]. In [17], a switchable rasorber/absorber based on slot arrays is investigated with a single polarization. When no bias voltage is applied on the diodes (off), the structure can operate as a rasorber. When a small voltage is applied on the diode (on), the transmission window would be moved to higher frequencies and even out of the absorption band. The rasorber then becomes an absorber accordingly. We hope that the passband can only exist or disappear, not just frequency shift. Meanwhile, the proposed device has dual-polarized performance. Detail design method and steps are provided in the following section.

## II. METHODS

*Step 1: Design of wideband graphene-based absorber:*

Graphene could be modeled as an infinitesimally thin surface [18], [19], which is characterized by a surface complex conductivity $\sigma$. The conductivity consists of intra and inter parts defined by Kubo's formulas. While only the intra-band contribution is considered in this paper since the proposed device works below 10 THz [20].

A wideband absorber based on graphene is designed in the first step, which is illustrated in Fig. 1. The absorber is constructed on a stacked two-layer substrate with an air gap. The distance between two substrates is nearly 1/4 wavelength of absorption frequency. The adopted substrate SiO2 with a dielectric of 3.8 and a thickness of 8 $\mu$m. The black section represents graphene. Eight graphene strips (with chemical potential of $\mu_{c1} = 1$ eV, relaxation time of $\tau_1 = 0.02$ ps) are embedded in the metallic strips of the absorber to provide the desired absorption at certain frequencies. The corresponding reflection coefficient is shown in Fig. 2(b). The simulated 10-dB impedance bandwidth is 107.3% from 0.285 to 0.945 THz. Note that the proposed design in this paper is simulated with the full-wave simulation tool, Ansoft HFSS.

*Step 2: Design of wideband absorber with graphene-based SRRs:*

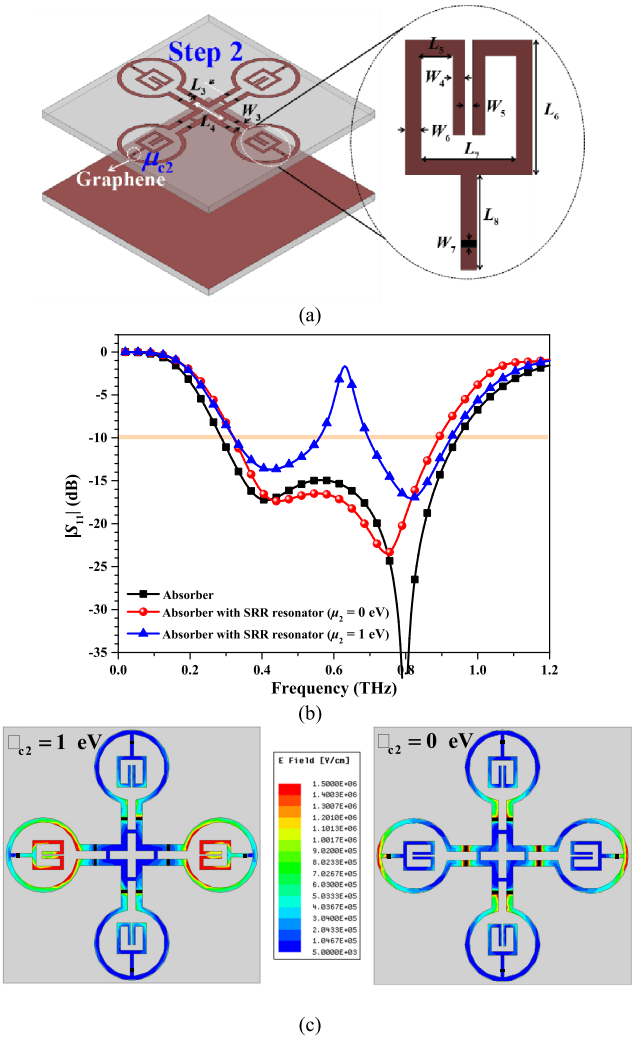


**FIGURE 2.** **(a) Configuration of the proposed absorber with SRRs based on graphene, (b) reflection coefficients of the proposed absorber with or without SRRs, and (c) electric field distribution on the resistive surface at 0.63 THz.**

Rasorber is a combination of radome and absorber, since it could function as an absorber at the stop-band, and be transparent at the transmission band. Means that a new path should be designed based on the pre-designed absorber within the absorption band. The energy of this selected frequency band should not be absorbed but be reflected since the existence of metal plate at the bottom. Hence, four SRRs connected with four metal-graphene hybrid strips are introduced to the absorber. The detailed structure of absorber with SRRs is displayed in Fig. 2(a). It should be mentioned that four graphene strips (with chemical potential of $\mu_{c2} = 1$ eV or 0 eV, relaxation time of $\tau_2 = 1$ ps) can be seen as switches, which could control on/off of SRRs by changing the chemical potential.

The reflection coefficients of the absorber with SRRs are shown in Fig. 2(b). When the chemical potential $\mu_{c2}$ is set to 0 eV, the reflection coefficients have two resonant points, forming the wideband performance. That is to say, the absorber with SRRs acts as a wideband absorber, just

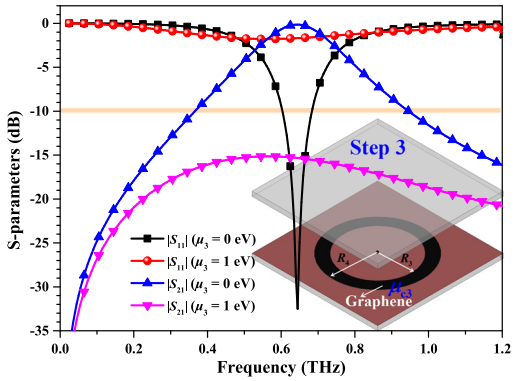


**FIGURE 3.** Configuration of the proposed graphene-based FSS with corresponding scattering parameters.

like the pre-designed absorber. When the chemical potential $\mu_{c2}$ is set to 1 eV, it is clear that a peak is occurred since the impedance is mismatched at 0.63 THz. From 0.56 to 0.695 THz, EM waves are mostly reflected rather than absorbed. The reason for reflection is due to the presence of metal plate in the second layer.

In order to further clarify the operation principle of the SRRs, electric field distribution of the upper surface, namely, resistive surface, are provided in Fig. 2(c). It can be observed that there is strong electric field distribution on SRRs at 0.63 THz when the chemical potential $\mu_{c2}$ is 1 eV. This indicates that the state of SRRs is "on" at this time. Thus, SRRs is the reason that makes reflection coefficient mismatch at 0.63 THz. While the chemical potential $\mu_{c2}$ is changed to 0 eV, only a few electric fields are distributed on the SRRs. That means that the state of SRRs is "off" at this moment. The SRRs have less impact on the performance of the absorber.

*Step 3: Design of graphene-based FSS:*

It is known that absorber only has absorption feature in the operating frequency band. To make the proposed rasorber have absorption-transmission-absorption response, a lossless path should be designed to bypass the lossy path. Reconfigurable FSS based on graphene is designed in this section. By replacing the metal sheet of absorber with SRRs to FSS, EM waves which be reflected in the above section could pass through the proposed design, forming the passband of the rasorber. In other words, the resistive sheet and bandpass FSS is nearly transparent to the incident EM waves. Note that the mismatched frequency band of the absorber with SRRs must coincide with the operating frequency of bandpass FSS. In the absorption band, the bandpass FSS should be nearly total-reflected and serve as a ground plane for the resistive sheet to absorb the incident waves.

The structure of the proposed FSS is plotted in Fig. 3 with corresponding scattering parameters. A graphene ring is embedded in the metal plate (with chemical potential of $\mu_{c3} = 0$ eV or 1 eV, relaxation time of $\tau_3 = 1$ ps). When the chemical potential $\mu_{c3}$ is set to 0 eV, the resonant frequency is at 0.63 THz with low insertion loss. Therefore, the proposed graphene-based FSS performs as

**TABLE 1.** Geometrical parameters ($\mu$m).

| $L_1$ | $L_2$ | $L_3$ | $L_4$ | $L_5$ | $L_6$ | $L_7$ | $L_8$ |
|---|---|---|---|---|---|---|---|
| 224 | 36 | 10 | 38.4 | 6.4 | 27.2 | 19.2 | 19.1 |
| $W_1$ | $W_2$ | $W_3$ | $W_4$ | $W_5$ | $W_6$ | $W_7$ | $R_1$ |
| 7.2 | 3.2 | 5.6 | 2.4 | 1.6 | 3.2 | 0.15 | 28.8 |
| $R_2$ | $R_3$ | $R_4$ | $D$ | $H$ | | | |
| 32.8 | 60 | 90 | 88 | 8 | | | |

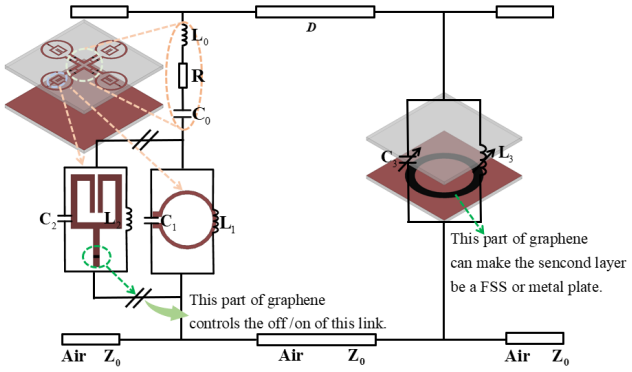


**FIGURE 4.** The equivalent circuit of the proposed switchable rasorber/absorber (Circuit parameters: $L_0 = 0.031$ nH, R = 300 Ohm, $C_0 = 0.0022$ pF, $C_1 = 0.0029$ pF, $L_1 = 0.2$ nH, $C_2 = 0.0064$ pF, $L_2 = 0.0071$ nH, $C_3 = 0.0038$ pF, $L_3 = 0.017$ nH).

an excellent bandpass FSS in this situation. Graphene has quasi-metal characteristic when the chemical potential $\mu_{c3}$ is changed to 1 eV. Therefore, the proposed graphene-based FSS functions as a metal plate in this case.

*Step 4: Design of switchable graphene-based rasorber/absorber :*

Combing the absorber with SRRs presented in step 2 and reconfigurable FSS proposed in step 3, we could achieve the final multi-functional design which could be seen in Fig. 4. By properly setting the value of the chemical potentials of graphene, the proposed device could be switched between the rasorber and absorber easily. The final geometrical parameters are listed in Table 1.

To further explain the operating mechanism of the proposed switchable rasorber/absorber, equivalent circuit is studied and depicted in Fig. 4. The hollow cross and graphene (act as resistors) with chemical potential of $\mu_{c1}$ in the center of the upper layer are modeled as a series RLC circuit. The circular ring resonator is equivalent to parallel circuit ($L_1$, $C_1$). SRR is also modeled as a parallel circuit ($L_2$, $C_2$). Graphene with chemical potential of $\mu_{c2}$ inserted in SRRs could control the SRRs work or be invalid. A graphene circular ring with chemical potential of $\mu_{c3}$ is embedded in the metal plate in the second layer, achieving a reconfigurable FSS which can be modelled as a parallel circuit ($L_3$, $C_3$). The reconfigurable FSS can function as FSS or metal plate by changing the chemical potential $\mu_{c3}$. The distance between two substrates D is nearly 1/4 wavelength of absorption frequency of 0.63 THz.

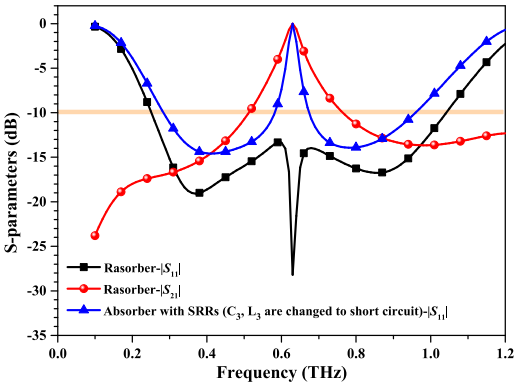


**FIGURE 5.** Scattering parameter of the proposed absorber with SRRs and rasorber simulated by ADS.

The equivalent circuit of the proposed switchable rasorber/absorber is simulated in Advanced Design System (ADS). It is found that the lower resonance of absorber is caused by the resistor R, inductance $L_0$, and the value of $D$. While the higher resonance of absorber is introduced by resistor R, inductances ($L_0$, $L_1$), and capacitances ($C_0$, $C_1$). Parallel circuit ($L_2$, $C_2$) is the reason that impedance mismatch at 0.63 THz. The reflection coefficient is shown in Fig. 5. The parallel circuit of $L_3$, $C_3$ is changed to short circuit when we simulate the absorber with SRRs using ADS. The scattering parameters of rasorber are illustrated in Fig. 5 as well. A new resonant point appears in the middle of the reflection coefficients due to the simultaneous resonance of $L_2$, $C_2$ and $L_3$, $C_3$.

## III. RESULTS

The final scattering parameters and the corresponding absorption rate of the proposed rasorber/absorber simulated by HFSS are displayed in Figs. 6(a-b) under TE polarization. Table 2 provides the configuration of chemical potentials.

From the Fig. 6(a), it is observed that a transmission window is achieved at 0.63 THz with the absorption rate of 0.1 when the chemical potentials $\mu_{c2}$ and $\mu_{c3}$ are 1 and 0 eV, respectively. Meanwhile, the simulated 10-dB impedance bandwidth is 110.2% from 0.275 to 0.95 THz, meaning that EM waves could pass through or be absorbed within this frequency band. $|S_{21}|$ above $-3$dB means that these part of EM waves could pass through the proposed design with low insertion loss. The characteristic of absorption-transmission-absorption is obtained. Therefore, the proposed design is called rasorber at this time.

From the Fig. 6(b), it is found that there is no transmission window when the chemical potentials $\mu_{c2}$ and $\mu_{c3}$ are 0 and 1 eV, respectively. The simulated 10-dB impedance bandwidth is 103.3% from 0.29 to 0.91 THz, meaning that EM waves could be absorbed within this frequency band. From the data of absorption rate, the proposed design has excellent absorptive ability. Therefore, the proposed design is called absorber at this time.

It is observed that the simulated results obtained by ADS and HFSS are highly consistent. Hence, the theoretical feasibility of the proposed design is further determined.

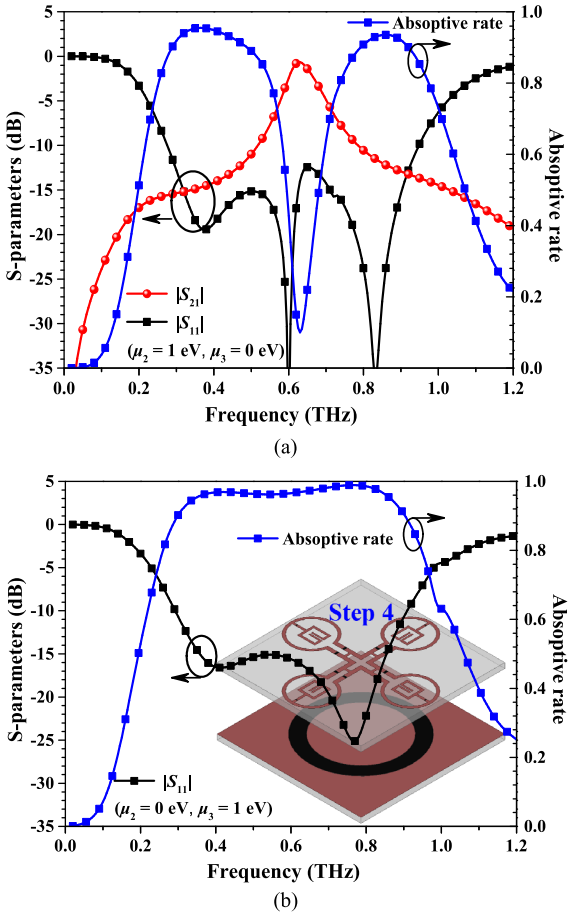


**FIGURE 6.** The configuration of the proposed graphene-based switchable rasorber/absorber with the corresponding scattering parameters and absorptive rate when the proposed design acted as a (a) rasorber or (b) absorber.

**TABLE 2.** Switchable rasorber/absorber with configuration of chemical potentials.

| Function | $\mu_{c1}$ (eV) | $\mu_{c2}$ (eV) | $\mu_{c3}$ (eV) |
|---|---|---|---|
| Rasorber | 1 | 1 | 0 |
| Absorber | 1 | 0 | 1 |

Rasorber and absorber could be switched easily by adjusting the values of chemical potentials, demonstrating that proposed device is multi-functional. Specific setting of graphene chemical potentials can be found in Table 2. In addition, the proposed rasorber and absorber are both insensitive to the polarization states of the incident EM waves at normal incidence due to the structural symmetry. The performance of the rasorber/absorber could be stable as the incident angle increases from 0° to 40°, which are not shown here for brevity.

To highlight the advantages of our proposed switchable rasorber/absorber, the performance comparison is tabulated in Table 3. It can be seen that our design has the merits of dual-polarization, wide band and multi-function.

In addition, graphene chemical potential can be tuned by applying a transverse electric field via a DC biased structure,

**TABLE 3.** The performance comparison.

| Refs | 10-dB Impedance Bandwidth | Lower/Upper Absorption Bandwidth | Polarization | Switchable rasorber/absorber |
|---|---|---|---|---|
| [10] | N.A. | Upper: 34.3% (4.8-6.81 GHz)[1] | Double | No |
| [11] | N.A. | Lower: 98.9% (2.4-7.1 GHz)[1] | Double | No |
| [12] | 130.5% (1.96-9.32 GHz) | Lower: 64.1% (1.92-3.73 GHz)[2]<br>Upper: 23% (7.41-9.34 GHz)[2] | Double | No |
| [16] | 72% (3.95 THz-8.4 THz) | Lower: 38.6% (3.45-5.1 THz)[2]<br>Upper: 26.1% (6.6-8.5 THz)[2] | Double | No |
| [17] | Rasorber: 106.2%<br>Absorber: 99.6% | N.A. (Only lower absorption band) | Single | Yes |
| **This paper** | **Rasorber: 110.2% (0.275-0.95 THz)**<br>**Absorber: 103.3% (0.29-0.91 THz)** | **Lower: 75% (0.25-0.55 THz)[2]**<br>**Upper: 27% (0.74-0.97THz)[2]** | **Double** | **Yes** |

[1]: 10 dB absorption band.
[2]: The bandwidths are for 80% absorption rate.
N.A.: No specific values.

and the experiment is demonstrated in [21], [22]. Therefore, the research results in the paper have theoretical and practical feasibility, simultaneously.

## IV. CONCLUSION

A double-polarization switchable rasorber/absorber is proposed in this paper. Detailed design guidelines and equivalent circuit are provided to explain the operating principle. When the proposed design acts as a rasorber, it has a transmission window with low insertion loss and two absorption bands at both sides of the passband. When the proposed design functions as an absorber, it has excellent absorption performance within a wide frequency band. Therefore, the device proposed in this paper has multi-functional characteristic. And it is quite suitable for stealth applications.

## REFERENCES

[1] A. Kondo, "Design and characteristics of ring-slot type FSS," *Electron. Lett.*, vol. 27, no. 3, pp. 240–241, Jan. 1991.
[2] M. Pazokian, N. Komjani, and M. Karimipour, "Broadband RCS reduction of microstrip antenna using coding frequency selective surface," *IEEE Antennas Wireless Propag. Lett.*, vol. 17, no. 8, pp. 1382–1385, Aug. 2018.
[3] J. P. Turpin, P. E. Sieber, and D. H. Werner, "Absorbing ground planes for reducing planar antenna radar cross-section based on frequency selective surfaces," *IEEE Antennas Wireless Propag. Lett.*, vol. 12, pp. 1456–1459, 2013.
[4] T. Tian, F. Zhou, and B. Zhao, "Multi-receiver deception jamming against synthetic aperture radar," in *Proc. CIE Int. Conf. Radar (RADAR)*, Oct. 2016, pp. 1–4.
[5] B. Li and Z. Shen, "Wideband 3D frequency selective rasorber," *IEEE Trans. Antennas Propag.*, vol. 62, no. 12, pp. 6536–6541, Dec. 2014.
[6] Y. Yu, Z. Shen, T. Deng, and G. Luo, "3-D frequency-selective rasorber with wide upper absorption band," *IEEE Trans. Antennas Propag.*, vol. 65, no. 8, pp. 4363–4367, Aug. 2017.
[7] H. Huang and Z. Shen, "Absorptive frequency-selective transmission structure with square-loop hybrid resonator," *IEEE Antennas Wireless Propag. Lett.*, vol. 16, pp. 3212–3215, 2017.
[8] X. Xiu, W. Che, Y. Han, and W. Yang, "Low-profile dual-polarization frequency-selective rasorbers based on simple-structure lossy cross-frame elements," *IEEE Antennas Wireless Propag. Lett.*, vol. 17, no. 6, pp. 1002–1005, Jun. 2018.
[9] S. Zhong, L. Wu, T. Liu, J. Huang, W. Jiang, and Y. Ma, "Transparent transmission-selective radar-infrared bi-stealth structure," *Opt. Express*, vol. 26, no. 13, pp. 16466–16476, Jun. 2018.
[10] W. Yu, G. Q. Luo, Y. Yu, Y. Pan, W. Cao, Y. Pan, and Z. Shen, "Dual-polarized band-absorptive frequency selective rasorber using meander-line and lumped resistors," *IEEE Trans. Antennas Propag.*, vol. 67, no. 2, pp. 1318–1322, Feb. 2019.
[11] Q. Chen, D. Sang, M. Guo, and Y. Fu, "Miniaturized frequency-selective rasorber with a wide transmission band using circular spiral resonator," *IEEE Trans. Antennas Propag.*, vol. 67, no. 2, pp. 1045–1052, Feb. 2019.
[12] X. Zhang, W. Wu, Y. Ma, C. Wang, C. Li, and N. Yuan, "Design dual-polarization frequency selective rasorber using split ring resonators," *IEEE Access*, vol. 7, pp. 101139–101146, 2019.
[13] M. Qu, S. Sun, L. Deng, and S. Li, "Design of a frequency-selective rasorber based on notch structure," *IEEE Access*, vol. 7, pp. 3704–3711, 2019.
[14] S. C. Bakshi, D. Mitra, and S. Ghosh, "A frequency selective surface based reconfigurable rasorber with switchable transmission/reflection band," *IEEE Antennas Wireless Propag. Lett.*, vol. 18, no. 1, pp. 29–33, Jan. 2019.
[15] Y. Wang, S.-S. Qi, Z. Shen, and W. Wu, "Tunable frequency-selective rasorber based on varactor-embedded square-loop array," *IEEE Access*, vol. 7, pp. 115552–115559, 2019.
[16] M. Qu and S. Li, "Graphene-based polarization insensitive rasorber with tunable passband," *Results Phys.*, vol. 14, Sep. 2019, Art. no. 102172.
[17] Y. Han, W. Che, X. Xiu, W. Yang, and C. Christopoulos, "Switchable low-profile broadband frequency-selective rasorber/absorber based on slot arrays," *IEEE Trans. Antennas Propag.*, vol. 65, no. 12, pp. 6998–7008, Dec. 2017.
[18] G. W. Hanson, "Dyadic green's functions for an anisotropic, non-local model of biased graphene," *IEEE Trans. Antennas Propag.*, vol. 56, no. 3, pp. 747–757, Mar. 2008.

[19] J. Chen, G. Hao, and Q.-H. Liu, "Using the ADI-FDTD method to simulate graphene-based FSS at terahertz frequency," *IEEE Trans. Electromagn. Compat.*, vol. 59, no. 4, pp. 1218–1223, Aug. 2017.
[20] J. Chen, J. Li, and Q. H. Liu, "Designing graphene-based absorber by using HIE-FDTD method," *IEEE Trans. Antennas Propag.*, vol. 65, no. 4, pp. 1896–1902, Apr. 2017.
[21] J. S. Gomez-Diaz, C. Moldovan, S. Capdevila, J. Romeu, L. S. Bernard, A. Magrez, A. M. Ionescu, and J. Perruisseau-Carrier, "Self-biased reconfigurable graphene stacks for terahertz plasmonics," *Nature Commun.*, vol. 6, no. 1, p. 6334, May 2015.
[22] L. Wang, I. Meric, P. Y. Huang, Q. Gao, Y. Gao, H. Tran, T. Taniguchi, K. Watanabe, L. M. Campos, D. A. Muller, J. Guo, P. Kim, J. Hone, K. L. Shepard, and C. R. Dean, "One-dimensional electrical contact to a two-dimensional material," *Science*, vol. 342, no. 6158, pp. 614–617, Nov. 2013.

**MEIJUN QU** (Student Member, IEEE) received the Ph.D. degree from the School of Information and Communication Engineering, Beijing University of Posts and Telecommunications (BUPT), Beijing, China, in 2020. She is currently a lecturer at Communication University of China, China. Her research interests include microwave passive component, antenna, metamaterial, and electromagnetic compatibility.

**TIANYU CHANG** is currently an Engineer with the International Department, The State Radio_monitoring_center Testing Center. He is also mainly engaged in SAR, MIMO OTA, and 5G terminal testing, standard setting, and related technology research.

**GAN GUO** is currently an Engineer and the Vice Chairman of wireless and mobile communication research field with the China Academy of Information and Communications Technology (CAICT), where he is also the Deputy Director of the China Telecommunication Technology Laboratory. His research interests include evaluation and verification method development and standardization of 3G, 4G, and 5G user equipment especially from physical layer to network layer.

**SHUFANG LI** (Senior Member, IEEE) received the Ph.D. degree from the Department of Electrical Engineering, Tsinghua University, Beijing, China, in 1997. She is currently the Director of the Ubiquitous Electromagnetic Environment Center of Education Ministry, China; and the Joint Laboratory, Beijing University of Posts and Telecommunications (BUPT); and the State Radio Monitoring Center (SRMC), China. She has published hundreds of articles interiorly and overseas, as well as several textbooks, translation works, and patents. Her research interests include the theory and design technology of radio frequency circuits in wireless communication, EMI/EMC, simulation technology and optimization for radiation interfere on high-speed digital circuit, and so on. She received the Young Scientists Reward sponsored by the International Union of Radio Science (URSI).